

SUPPLEMENTARY TABLES AND FIGURES

Supplementary Table 1. qPCR gene-specific Primer sequences

Gene	Forward Primer (5'-3')	Reverse Primer (5'-3')
<i>SLC26A3</i>	CAGCCCCCTATTACACCTGA	CCTCCTGTGCTCTCCTGAAC
<i>SLC26A6</i>	GCCTTGAACGACTCCATGAT	TGTGAGACGAAGACCTGCAC
<i>CFTR</i>	CCTATGACCCGGATAACAAGGA	GAACACGGCTTGACAGCTTTA
<i>SLC9A3</i>	CCTGACCATCAAGCCTCTGG	ACATTCAGGATCCGGTCTCG
<i>LGR5</i>	GATGTTGCTCAGGGTGGACT	GGGAGCAGCTGACTGATGTT
<i>GUCY2C</i>	GGCTGTCTTTAGTTCCCAGG	GAAAGTAGCGTTCACAGTCACAT
<i>MYO6</i>	TAACCCACTCCTAGAAGCCTTT	GCACCAGCACACAACCTATAA
<i>GAPDH</i>	GAAGGTGAAGGTCGGAGTC	GAAGATGGTGATGGGATTTTC

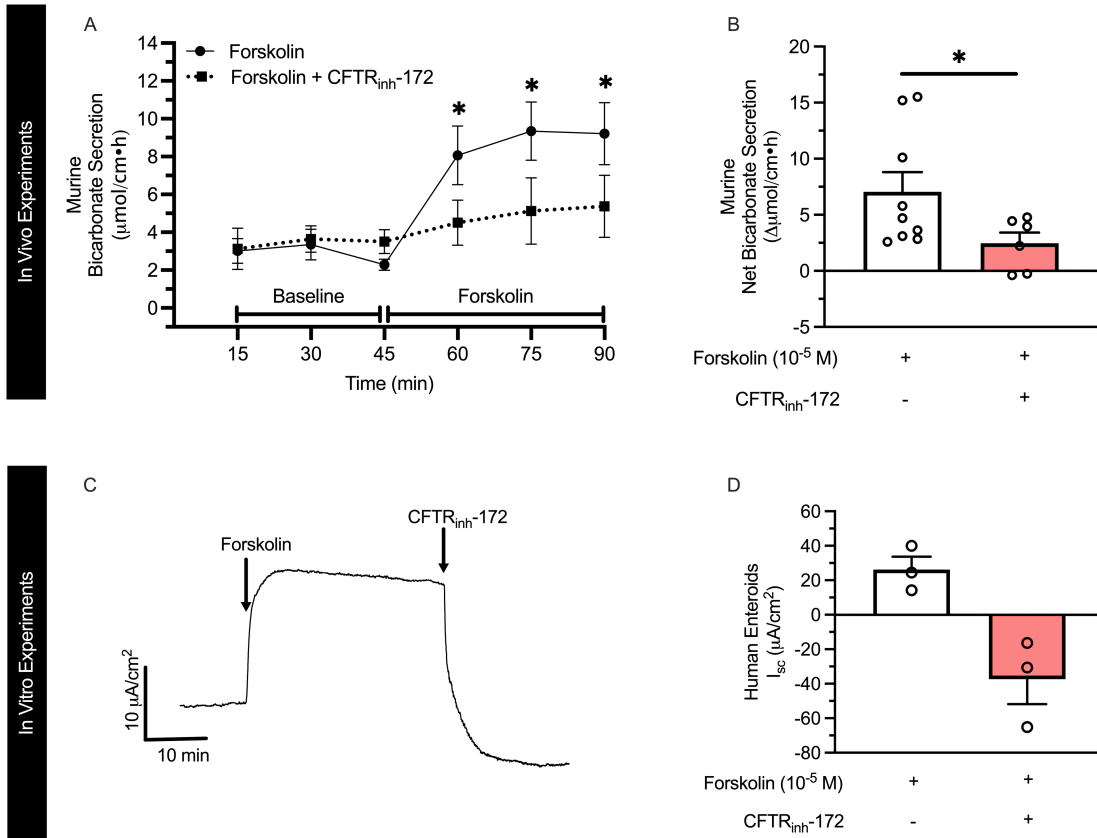
SLC26A3 (down-regulated in adenoma, DRA), *SLC26A6* (putative anion transporter-1, PAT-1), *CFTR* (cystic fibrosis transmembrane conductance regulator), *SLC9A3* (sodium/hydrogen exchanger 3, NHE3), *LGR5* (leucine rich repeat containing G protein-coupled receptor 5), *GUCY2C* (guanylate cyclase 2C), *MYO6* (myosin VI), *GAPDH* (glyceraldehyde-3-phosphate dehydrogenase)

Supplementary Table 2. List of antibodies

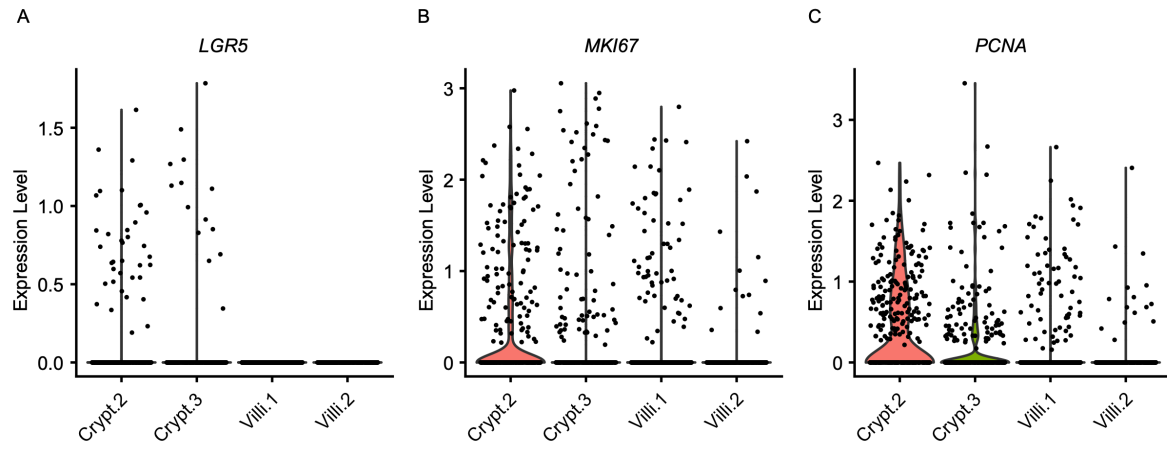
Primary Antibodies	Dilution	Manufacturer
DRA (mouse)	1:200	Santa Cruz (sc-376187)
NHE3 (rabbit)	1:400	Novus Biologicals (NBP1-82574)
Villin (rabbit)	1:400	ThermoFisher (PA5-29078)
Villin (mouse) 1D2C3	1:200	Santa Cruz (sc-58897)
Hoechst 33342	Per manufacturer's protocol	Abcam (ab228551)

Secondary antibodies	Dilution	Manufacturer
Goat Anti-Rabbit Alexa flour 594	1:300	Abcam (ab150088)
Goat Anti-Mouse Alexa flour 647	1:300	Abcam (ab150115)
Goat Anti-Mouse IgG H&L (Alexa Fluor® 488)	1:1000	Abcam (ab150113)

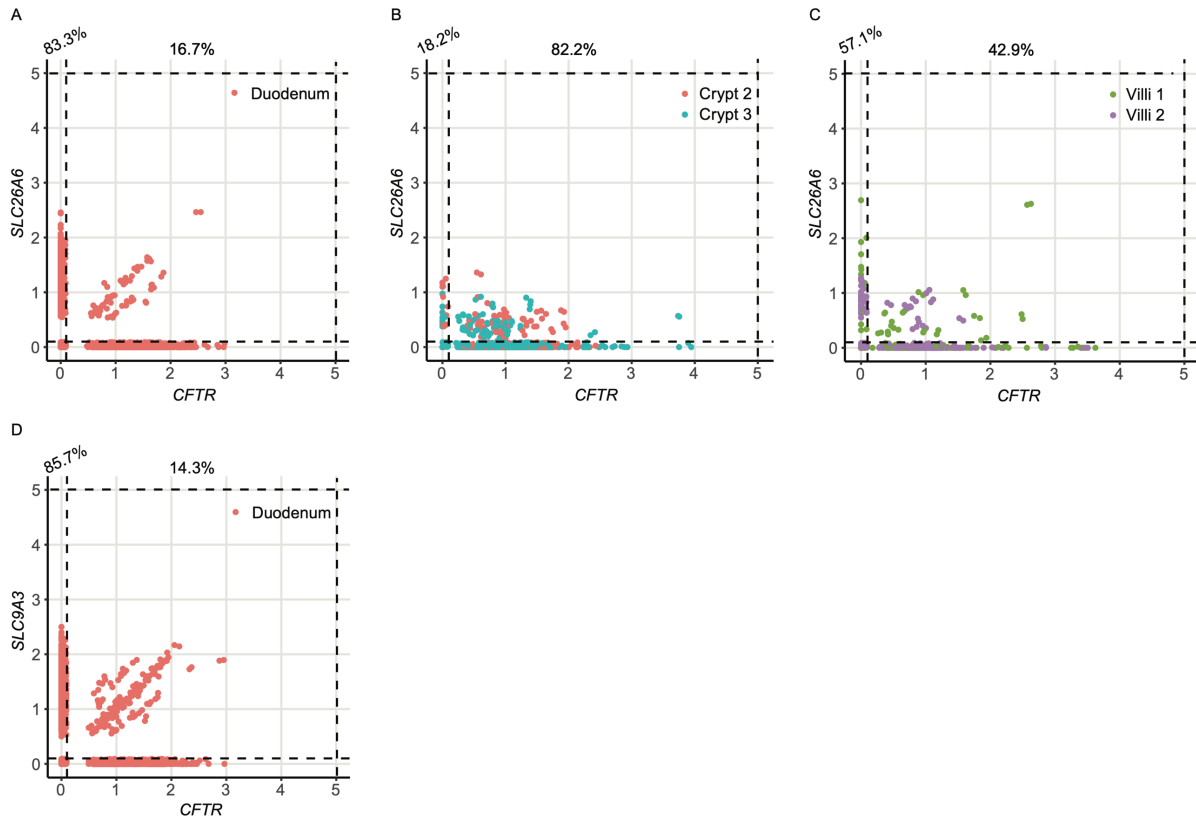
SUPPLEMENTARY FIGURES



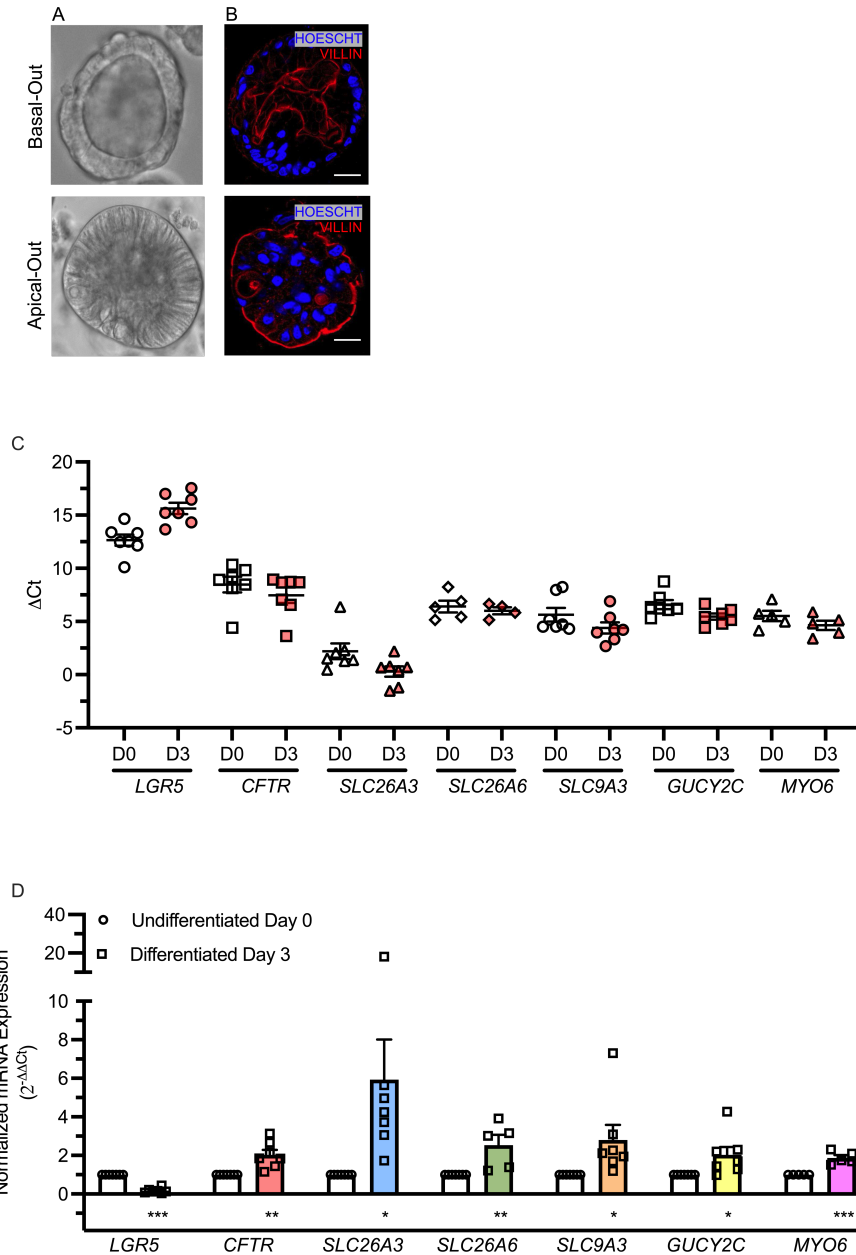
Supplemental Figure 1. CFTR_{inh}-172 inhibits forskolin-stimulated duodenal bicarbonate secretion in mice and human enteroids. **A.** To compare the effect of pharmacologic CFTR inhibition with CFTR_{inh}-172 on linacotide and forskolin-stimulated bicarbonate secretion, we performed similar in vivo experiments as Figure 2A. Duodenum of wildtype mice were perfused with saline then forskolin (10⁻⁴ M) (black circles) or saline + CFTR_{inh}-172 (2 x 10⁻⁵ M) then forskolin (10⁻⁴ M) (black squares). Bicarbonate secretion was calculated from the perfusates similar to Figure 2A. *, P<0.05 by one-way ANOVA. **B.** Comparison of net change in forskolin-stimulated bicarbonate secretion (peak response – baseline secretion) in the presence or absence of CFTR_{inh}-172. Columns with whiskers represent mean \pm SEM with each circle representing a different experiment. Mean \pm SEM percent inhibition indicated above columns. *, P<0.05 by unpaired two-tailed Student's t-test. **C.** Representative trace of forskolin (10⁻⁵ M, basolateral)-stimulated short-circuit current, followed by inhibition by CFTR_{inh}-172 (2 x 10⁻⁵ M, basolateral), in undifferentiated human duodenal enteroids monolayers. **D.** Quantification of replicate experiments performed in C. Columns with whiskers represent mean \pm SEM with each circle representing a different experiment.



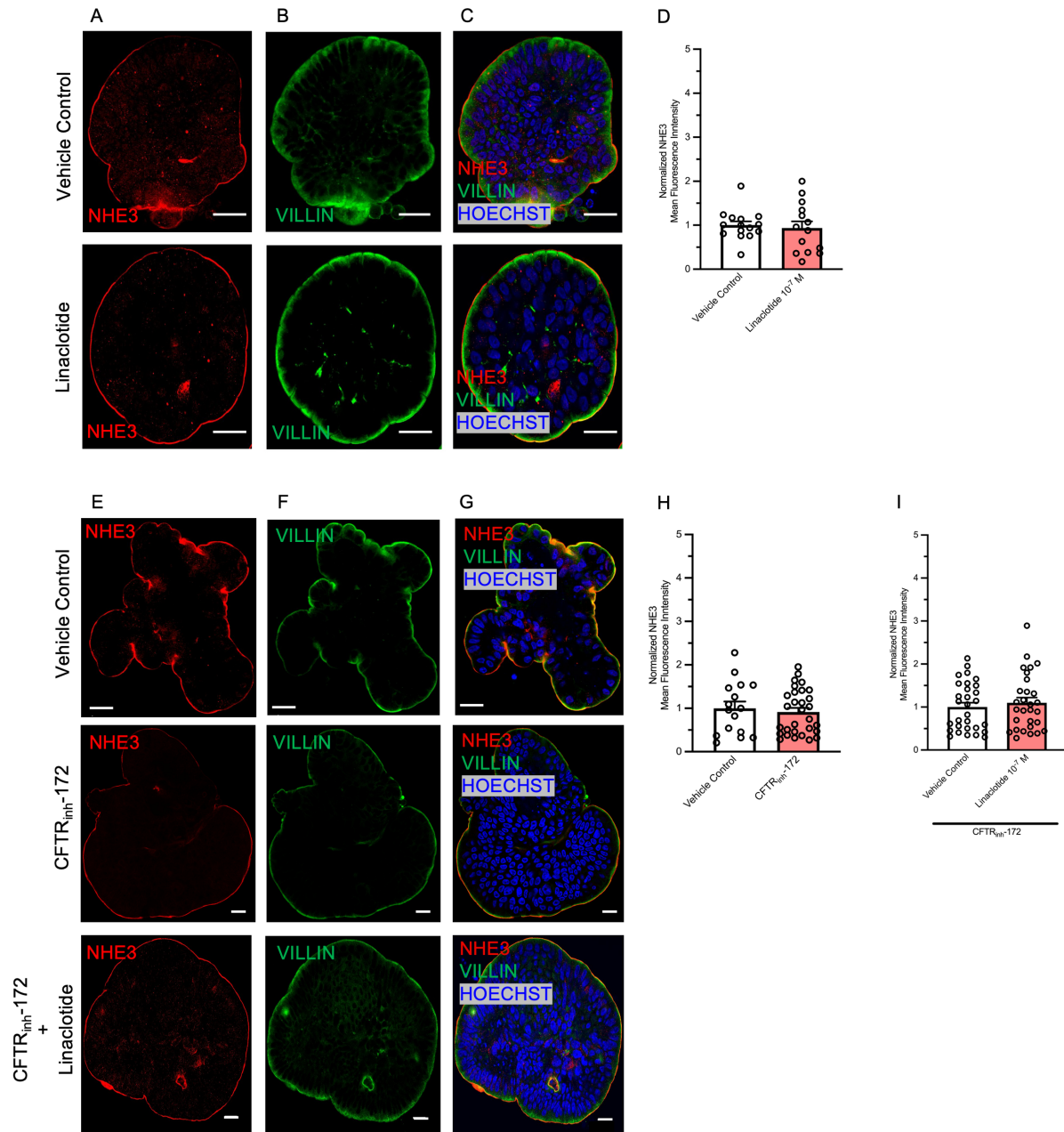
Supplementary Figure 2. Validation of previously published human duodenum scRNA-seq datasets. A-C. To verify the crypt vs. villi identity in the Busslinger et al. dataset we examined the expression of *LGR5* (A), *MKI67* (B), and *PCNA* (C).



Supplementary Figure 3. Co-expression of *CFTR* and *SLC26A6* (PAT-1) and *SLC9A3* (NHE3) from human duodenal sc-RNaseq data. A-C. Co-expression of *SLC26A6* (PAT-1) and *CFTR* mRNA using FeatureScatter based on Elmentaite et al.¹⁴ enterocytes (A) and Busslinger et al.¹⁵ crypt and villi (B and C) datasets. **D.** Co-expression of *SLC9A3* (NHE3) and *CFTR* mRNA using FeatureScatter based on Elmentaite et al. enterocytes. There were insufficient numbers of *SLC9A3* positive cells in the Busslinger et al. dataset to do the same analysis as B and C. Numbers on top of graphs represent the percentage of *SLC26A6*- or *SLC9A3*-expressing cells that express these only (left) or *SLC26A6*/*SLC9A3* and *CFTR* (right).



Supplementary Figure 4. Characterization of Apical-Out Duodenal Enteroids. **A.** Sample brightfield microscope images of basal-out (top) and apical-out (bottom) human duodenal enteroids. **B.** Representative confocal immunofluorescent images of basal-out (top) and apical-out (bottom) human duodenal enteroids stained with villin (apical membrane) and Hoescht (cell nucleus). Scale bar = 20 μm . **C and D.** mRNA expression of *LGR5*, *CFTR*, *SLC26A3*, *SLC26A6*, *SLC9A3*, *GUCY2C*, and *MYO6* in undifferentiated and differentiated (x3 days) apical-out human duodenal enteroids. Delta CT was calculated by comparing to *GAPDH* expression (C) and Delta Delta CT was calculated by comparing Differentiated Day 3 enteroids to Undifferentiated Day 0 enteroids. *, $P < 0.05$; **, $P < 0.01$; ***, $P < 0.001$ compared to Undifferentiated Day 0 enteroids by unpaired two-tailed Student's t-test.



Supplemental Figure 5. Linaclotide does not change the membrane expression of NHE3 in apical-out human duodenal enteroids. **A-C.** Representative confocal microscopy images of NHE3 (A), villin (B), and NHE3 and villin and Hoescht (C) during control conditions (water, 40 minutes, top) or linaclotide (10^{-7} M, 40 minutes, bottom). **D.** Quantification of NHE3 present at the apical membrane using villin to define apical membrane, similar to Fig. 6. **E-G.** Representative images for apical membrane NHE3 mean fluorescence intensity following CFTR_{inh}-172 (2×10^{-5} M, 40 minutes) with or without linaclotide (10^{-7} M, 40 minutes) treatment. **H-I.** Quantification of images, normalized to vehicle controls for comparison. Vehicle control for linaclotide was water and for CFTR_{inh}-172 was DMSO. Columns with whiskers are mean \pm SEM with each dot representing a different enteroid. Enteroids from three different patients were used for each condition. Significance determined by unpaired two-tailed Student's t-test. For enteroids treated with both CFTR_{inh}-172 and linaclotide, enteroids were pretreated with CFTR_{inh}-172 for 40 minutes prior to linaclotide treatment.